Multi-modal commutative dynamics in semi-crystalline polymers undergoing multiple shape memory behavior

Xiaodong Wang[1], Haibao Lu[1,5], Galina Gorbacheva[2,5], Mokarram Hossain[3] and Yong Qing Fu[4]

[1]National Key Laboratory of Science and Technology on Advanced Composites in Special Environments, Harbin Institute of Technology, Harbin 150080, P.R. China

[2]Mytishchi Branch of Federal State Budgetary Educational Institution of Higher Education, Bauman Moscow State Technical University, Mytishchi 141005, Russia

[3]Zienkiewicz Centre for Computational Engineering, College of Engineering, Swansea University, Swansea, UK

[4]Faculty of Engineering and Environment, Northumbria University, Newcastle upon Tyne NE1 8ST, UK

[5]E-mail: luhb@hit.edu.cn and gorbacheva@mgul.ac.ru

Abstract: Semi-crystalline polymers offer great opportunities for design and tuning of multi-shape memory effect (multi-SME) through their programmable melting transitions. However, coexistence of amorphous and crystalline components as well as their multiple interfaces results in complex cooperative dynamics. In this study, we propose a one-dimensional (1D) multi-modal dynamic model to describe the commutative and cooperative dynamics in semi-crystalline shape memory polymers (SMPs) undergoing multi-SME. A three-phase model and Takayanagi principle are firstly applied to study the cooperative dynamics of amorphous/crystalline components and their interfaces. Phase transition theory and modified Avrami theory

are further used to model the cooperative dynamics of glass and melting transitions, respectively. Commutative dynamics and glass/melting transitions are further investigated to achieve custom-designed multi-SME and shape recovery behaviors. Finally, effectiveness of the newly established model was demonstrated to predict triple-SMEs and quadruple-SMEs in semi-crystalline polymers reported in literature, and the theoretically obtained results show good agreements with the experimental ones.

Keywords: Semi-crystalline polymer, commutative dynamics, shape memory effect

1. Introduction

Shape memory polymer (SMP) is one of the most popular soft matters and has the capabilities of recovering its highly pre-deformed shapes in response to external stimuli, such as heat, solvent, light, electric or magnetic fields [1-6]. Different from the conventional shape-change soft matters, the SMP can have a temporarily fixed shape and then regain its permanent shape due to its special thermodynamics. Therefore, it has a great numbers of practical applications for biomedical devices, textiles, actuators and drug delivery systems [7-11].

Unlike the conventional “dual-stage SMP” which has a single transition zone and can only fix one temporary shape, multi-stage SMPs are capable of fixing two or more temporary shapes in the sequentially programmed processes [10], and then regain their temporary multiple shapes upon step-by-step thermal or other stimulations. To achieve this, the multi-stage SMPs are necessary to have two or more

shape-fixing mechanisms distinguished by their different thermal transitions [12]. Among various types of multi-stage SMPs, semi-crystalline polymers are the most common material systems [13-15], since they easily display two well-separated transitions, e.g., one from the glass transition of amorphous component and the other from the melting transition of the crystalline component [16]. Moreover, quadruple-SMEs were also discovered in such material systems by incorporating poly(L-lactic acid) (PLLA) and poly(D-lactic acid) (PDLA) into a polyurethane matrix, and such triblock polymers have two glass transitions and two melting transitions which are used to generate different temporary shapes [17].

However, majority of the previous studies have been focused on the amorphous SMPs, using the classic phase transition theory [18,19] and Maxwell models [20,21]. Due to their complex morphology and internal structures, the relaxation behavior of semi-crystalline polymers is really hard to model. Not only the glass transition of amorphous component, but also the melting transition of crystalline component should be considered. According to the three-phase model [22], the semi-crystalline polymers have three components, e.g., the mobile amorphous component, rigid amorphous component and crystalline component. The rigid amorphous component is the amorphous segments which are within the spherulitic structures, and it has no contribution to the glass transition event [23]. Meanwhile, relaxation of the mobile amorphous component is resulted from the cooperative motions of their neighbors and interspaces [24]. Whereas the crystalline component significantly confines the relaxation motions, thus plays an essential role to influence the glass transition [25].

Establishing the constitutive models of the semi-crystalline polymers is crucial to reveal the working mechanisms of viscoelastic relaxation behavior. Ge et. al utilized multi-branched models to explain the finite deformation and recovery behavior of semi-crystalline polymers [26,27]. Moon et. al did finite element analysis using Abaqus to study triple-shape recovery behavior of a semi-crystalline stent [28]. However, the cooperative dynamics between crystalline and amorphous components has not been considered in most of these previous reports. Therefore, it is critical to propose an effective and theoretical approach to characterize the intrinsic molecular structure and thermodynamics, in order to identify their working principles.

In this study, a 1D multi-modal dynamic model is firstly developed to explain the unique relaxation characteristics of semi-crystalline SMPs. Based on the three-phase model [22] and the Adam-Gibbs theory [29,30], the constitutive relationship between the relaxation of mobile amorphous component and the degree of crystallinity is formulated as a function of glass transition temperature (T_g) of semi-crystalline SMPs. The modified Avrami theory [31] is then introduced to describe the melting transition and thermodynamics of crystalline components. Furthermore, rigid amorphous component is introduced into the interfaces between mobile amorphous and crystalline components, and effect of three components on the thermomechanical behavior are formulated using the multi-modal commutative and cooperative models, to characterize the thermodynamics and recovery behavior of the semi-crystalline SMPs [32,33]. Finally, the obtained analytical results are compared with the experimental ones reported in Ref. [17,34] in order to verify the newly proposed

model.

2. Modelling and simulation

2.1 Extended three-phase model

Thermomechanical behavior of semi-crystalline SMPs is strongly dependent on their morphologies [35]. Based on the three-phase model [22], the semi-crystalline SMPs are composed of three parts, i.e. crystalline, mobile amorphous and rigid amorphous components, the last of which is located at the interfacial regions between the crystalline and mobile amorphous ones, as shown in Figure 1. To characterize these unique three-phase features in the semi-crystalline SMPs, Takayanagi principle is employed to describe the storage modulus ($E(T)$) as following [32],

$$E(T) = 1/\left(\frac{\lambda}{\varphi E_c(T) + (1-\varphi) E_r(T)} + \frac{1-\lambda}{E_m(T)} \right) \tag{1}$$

where E_c, E_r and E_m are the storage moduli of the crystalline, rigid amorphous and mobile amorphous components, respectively, λ and φ are the dimensionless width and length of crystalline component along the loading direction, respectively.

[Figure 1]

In Equation (1), the parameters λ and φ are used to characterize the volume fractions of three components in the semi-crystalline polymers, and they can be determined using a temperature modulated differential scanning calorimetry (TMDSC) method [36]. The volume fractions of these three components can be written as,

$$W_m = \frac{\Delta C_p}{\Delta C_{p0}} = 1\text{-}\lambda \; ; \; W_c = \frac{\Delta h}{\Delta h_0} = \lambda\varphi \; ; \; W_r = 1 - W_m - W_c = \lambda(1-\varphi) \tag{2}$$

where W_m, W_r and W_c are the volume fractions of the mobile amorphous, rigid amorphous and crystalline components, respectively. ΔC_p and ΔC_{p0} are the heat capacities of the semi-crystalline and pure amorphous polymers, respectively. Δh and Δh_0 are the heights of melting peaks of the semi-crystalline and pure amorphous polymers, respectively, from the experimental results of the TMDSC [37].

According to the equations (1) and (2), the thermomechanical behavior of semi-crystalline SMPs is critically determined by the parameters of λ and φ, whereas the thermomechanical glass and melting transitions are essentially determined by these two parameters, according to the Takayanagi principle [32]. Therefore, effects of glass and melting transitions on the thermomechanical behavior of semi-crystalline SMPs will be investigated in the following section.

2.2 Glass transition of the mobile amorphous component

In the semi-crystalline SMPs, the mobile amorphous component enables the polymer with shape memory effect (SME) due to its glass transition. Phase transition theory has then been employed to study the effect of glass transition of amorphous component on the SME in semi-crystalline SMP [38]. The phase evolution function (ϕ_m) has the following relationship with temperature (T) and time (t) [38],

$$\phi_m(T) = \frac{\varepsilon_{s,m}}{\varepsilon_{pre,m}} = \left(1 - \exp\left(-\frac{\Delta H(T)}{k_b T}\right)\right)^{\frac{t}{\tau_0}} \quad (t = (T - T_i)/q) \tag{3}$$

where $\varepsilon_{s,m}$ is the stored strain, $\varepsilon_{pre,m}$ the pre-deformed strain, $\Delta H(T)$ is the activation energy, k_b is the Boltzmann's constant, τ_0 is the internal relaxation time, T_i is the initial temperature and q is the heating rate.

On the other hand, the confinement effect of crystalline component on the glass transition of mobile amorphous component should also be considered in the semi-crystalline SMPs, and their glass transition behaviors are different from those of the pure amorphous SMPs. According to the Adam-Gibbs theory [30], the cooperative rearranging region (CRR) is introduced to describe the cooperative phase transition of mobile amorphous and crystalline components. The domain size ($z(T)$), which indicates the number of the components in a CRR, can be expressed as [39],

$$z(T) = \frac{\ln 2 N k_b T_g}{\Delta C_p (T - T_0)} \tag{4}$$

where N is the overall number of components, T_g is the glass transition temperature of mobile amorphous component, and T_0 is the low-temperature limit where the configuration energy becomes infinitesimal.

Substituting equation (2) into (4), the expression of domain size ($z(T)$) as functions of temperature and volume fraction for the mobile amorphous component is obtained,

$$z(T) = \frac{\ln 2 N k_b T_g}{W_m \Delta C_{p0} (T - T_0)} \tag{5}$$

The relaxation time ($\tau(T)$) of the mobile amorphous component can then be derived from the Adam-Gibbs theory [30],

$$\tau(T) = \tau^* \exp\left(\frac{\Delta\mu}{R} \left(\frac{z(T)}{T} - \frac{1}{T^*} \right) \right) = \tau^* \exp\left(\frac{\Delta\mu}{R} \left(\frac{\ln 2 N k_b T_g}{W_m \Delta C_{p0} T (T - T_0)} - \frac{1}{T^*} \right) \right) \tag{6}$$

where $\Delta\mu$ is the activation energy of per mole mobile amorphous component, R is the gas constant and τ^* is the relaxation time at temperature T^*.

To further model the phase transition, it is necessary to develop a framework between the activation energy ($\Delta H(T)$) and volume fraction of the mobile amorphous

component. According to the Adam-Gibbs theory [30] and equation (5), the activation energy ($\Delta H(T)$) can be rewritten as,

$$\Delta H(T) = z\Delta\mu = \frac{\ln 2 N k_b T_g \Delta\mu}{W_m \Delta C_{p0}(T - T_0)} \tag{7}$$

Combining equations (3) and (7), the phase evolution function (ϕ_m) of the mobile amorphous component has the following constitutive relationship with temperature and volume fraction,

$$\phi_m(T,t) = \frac{\varepsilon_{s,m}}{\varepsilon_{pre,m}} = \left(1 - \exp\left(-\frac{\ln 2 N T_g \Delta\mu}{W_m \Delta C_{p0} T (T - T_0)}\right)\right)^{\frac{t}{\tau_0}} \tag{8}$$

2.3 Melting transition of crystalline component

For the melting transition of crystalline component, the Avrami theory [31] is oftn used to characterize the dynamic transition behavior of the semi-crystalline SMP at the melting transition temperatures (T_m). Here the phase evolution function (ϕ_c) of the crystalline component is determined by the stored strain ($\varepsilon_{s,c}$) and pre-deformed strain ($\varepsilon_{pre,c}$) of the crystalline component in semi-crystalline SMPs, which can be written using the following equation [31],

$$\phi_c(T,t) = \frac{\varepsilon_{s,c}}{\varepsilon_{pre,c}} = \exp\left(-\int_0^t K(T(t))dt\right) \tag{9}$$

where $K(T(t))$ is the kinetic parameter of the melting transition. Based on the Jeziorny method [40], this kinetic parameter is determined by the temperature ($T(t)$),

$$K(T) = K_{\max} \exp(-4\ln 2 (T - T_m)^2 / D^2) \tag{10}$$

where $K_{\max}$ is the maximum value of kinetic parameter and D is a constant [40].

Substituting equation (10) into (9), the phase evolution function of the crystalline

component can be rewritten as,

$$\phi_c(T,t)=\frac{\varepsilon_{s,c}}{\varepsilon_{pre,c}}=\exp\left(-K_{\max}\int_0^t \exp(-4\ln 2(T-T_m)^2/D^2)dt\right) \tag{11}$$

The stored strain (ε_s) of semi-crystalline SMP is a combination of those of the mobile amorphous ($\varepsilon_{s,m}$) and crystalline ($\varepsilon_{s,c}$) components. Therefore, the stored strain (ε_s) can be obtained based on the equations (8) and (11),

$$\varepsilon_s(T,t)=\varepsilon_{s,m}+\varepsilon_{s,c}=\phi_m(T,t)\varepsilon_{pre,m}+\phi_c(T,t)\varepsilon_{pre,c} \tag{12}$$

2.4 Dynamic thermomechanical behavior of semi-crystalline SMP

As discussed in Ref. [41], the storage modulus of the mobile amorphous component (E_m) as a function of temperature can be written as,

$$E_m(T)=E_{m,f}\left(1+\frac{(1-\phi_m(T))(E_{m,a}/E_{m,f}-1)}{1+\alpha\phi_m(T)(E_{m,a}/E_{m,f}-1)}\right) \tag{13}$$

where $E_{m,f}$ and $E_{m,a}$ are the storage moduli of the frozen and active phases in the mobile amorphous component, respectively [41], and α is a fitting constant.

Based on a previous study of the semi-crystalline SMPs [26], the crystalline components cannot resist the external force after their melting transitions. Therefore, we can further modify the relationship of the storage modulus of the crystalline component (E_c) and temperature (T),

$$E_c(T)=E_{c0}\phi_c(T,t)=E_{c0}\exp\left(-K_{\max}\int_0^t \exp(-4\ln 2(T-T_m)^2/D^2)dt\right) \tag{14}$$

where E_{c0} is the storage modulus of the pure crystalline component before the melting transition.

In the semi-crystalline SMP, the rigid amorphous component works at the interfaces between mobile amorphous and crystalline components, thus enabling their

cooperative relaxation motions. Once the crystalline component undergoes the melting transition at T_m, the rigid amorphous component is released from the crystalline component and thus will have the same relaxation motion as that of the mobile amorphous component. Therefore, the storage modulus of the rigid amorphous component ($E_r(T)$) can be expressed using the following relationship,

$$E_r(T) = E_{r0}\phi_c(T,t) + E_{m,a}(1-\phi_c(T,t)) \tag{15}$$

where E_{r0} is the initial storage modulus of the rigid amorphous component.

By substituting equations (13), (14) and (15) into equation (1), the storage modulus of semi-crystalline SMPs can be finally obtained as,

$$\frac{1}{E(T)} = \frac{\lambda}{\varphi E_{c0}\phi_c(T,t) + \varphi E_{r0}\phi_c(T,t) + (1-\varphi)E_r(T)} + \frac{1-\lambda}{E_m(T)} \tag{16}$$

2.5 Multiple melting transitions in semi-crystalline SMP

In the semi-crystalline SMP, the multiple melting transitions could provide many temporary shapes and enable them with multi-SME. Based on the Boltzmann's superposition principle [42], equation (12) can be further extended as,

$$\varepsilon_s(T,t) = \sum_{i=1}^{n}\varepsilon_{s,m}(i) + \sum_{k=1}^{m}\varepsilon_{s,c}(k) = \sum_{i=1}^{n}\phi_m(i)\varepsilon_{pre,m}(i) + \sum_{k=1}^{m}\phi_c(k)\varepsilon_{pre,c}(k) \tag{17}$$

where *n* and *m* are the numbers of glass and melting transitions in the semi-crystalline SMP, respectively. Parameters *i* and *k* indicate the *i*th glass transition component and the *k*th melting transition component, respectively.

According to the Takayanagi principle [32], the storage modulus of a semi-crystalline SMP can be obtained by expansion of equation (16),

$$\frac{1}{E(T)} = \sum_{i=1}^{n}\frac{\lambda_m(i)}{E_m(i)} + \sum_{k=1}^{m}\frac{\lambda_c(k)}{\phi_c(k)E_c(k) + \phi_c(k)E_r(k) + (1-\phi_c(k))E_r(k)} \tag{18}$$

2.6 Temperature memory effect (TME) in semi-crystalline SMP

According to the previous studies [43,44], the programming thermomechanical history has a significantly effect on the shape memory behavior of SMP. The TME has been identified as the capability of amorphous SMP to memorize the deformation temperature (T_d), which plays an essential role to determine the recovery temperature. Therefore, study on the TME is critical to describe the thermodynamics in SMP.

Based on the phase transition theory [38], the mobile amorphous component is composed of both the active and frozen phases. During the glass transition, there is a phase transition from the frozen phase into the active one with an increase in temperature. Generally, this constitutive stress-strain relationship is governed by the multi-branch Maxwell model [45],

$$\sigma_m(T,t)=(1-\phi_m(T,t))E_{m,a}\varepsilon_m(t)+\phi_m(T,t)E_{m,f}\int_0^t \frac{d\varepsilon_m(s)}{dt}\exp\left(-\frac{t-s}{\tau(T)}\right)ds \qquad (19)$$

where $\sigma_m(T,t)$ and $\varepsilon_m(s)$ are the stress and strain at the time *s*, respectively.

On the other hand, it is necessary to establish the constitutive stress-strain relationships for the rigid amorphous and crystalline components, which work as another branch in the multi-branch model. In the previous work [46], experimental results revealed that there are too many voids between the amorphous and crystalline components during large deformations of the semi-crystalline polyamide 6 (PA 6). In this study, a small deformation of semi-crystalline SMPs is considered, therefore, we can assume that there are no voids generated from the rigid amorphous component. This will be induced by the strong bonding between mobile amorphous and crystalline components [47,48]. Here the stress of the rigid amorphous component can be written

as [47,48],

$$\sigma_r(T,t) = \sigma_y(T,\dot{\varepsilon}_r)\phi_c(T,t)(1-\exp(-A\dot{\varepsilon}_r t)) \tag{20}$$

where $\dot{\varepsilon}_r$ and σ_y are the strain rate and yielding stress of the rigid amorphous component, respectively.

According to the compensation law [49], the yielding stress ($\sigma_y(T,\dot{\varepsilon}_r)$) of semi-crystalline polymer as a function of strain rate ($\dot{\varepsilon}_r$) can be expressed as,

$$\frac{\sigma_y(T,\dot{\varepsilon}_r)}{T} = \frac{\sigma_i(0)-\left(\sigma_i(0)T/T^*\right)}{T} + \frac{2.3k_b}{V}\log\left(\dot{\varepsilon}_r/\dot{\varepsilon}_{r0}\right) \tag{21}$$

where $\sigma_i(0)$ is the internal stress at T =0 K and $\dot{\varepsilon}_{r0}$ is the referenced strain rate.

At a finite strain, it is assumed that the stress of crystalline component follows neo-Hookean principle, thus it can be obtained by Cauchy stress (σ_c) function [26],

$$\sigma_c = \sigma_r(T,t) = \mu_c\phi_c(T)\left((\varepsilon_c+1)^2 - 1/(\varepsilon_c+1)\right) \tag{22}$$

where μ_c is the shear modulus of the crystalline component. Since the rigid amorphous component is in a series connection with the crystalline component, as $\sigma_c = \sigma_r(T,t)$.

According to the Takayanagi principle [32], the formulate of the stress (σ) and strain (ε) for the semi-crystalline SMP can be obtained,

$$\sigma(T,t) = 1/\left(\sum_{i=1}^{n}\frac{\lambda_m(i)}{\sigma_m(i)} + \sum_{k=1}^{m}\frac{\lambda_c(k)}{\sigma_c(k)}\right) = 1/\left(\sum_{i=1}^{n}\frac{\lambda_m(i)}{\sigma_m(i)} + \sum_{k=1}^{m}\frac{\lambda_c(k)}{\mu_c(k)\phi_c(k)\left((\varepsilon_c(k)+1)^2 - 1/(\varepsilon_c(k)+1)\right)}\right) \tag{23a}$$

$$\varepsilon(T,t) = \varepsilon_m(i) = (1-\varphi_c(k))\varepsilon_r(k) + \varphi_c(k)\varepsilon_c(k) \tag{23b}$$

3. Results and discussion

3.1 Cooperative dynamics in semi-crystalline SMP

In this section, the above proposed models are utilized to investigate the

thermomechanical behaviors of the semi-crystalline SMPs. Based on the proposed model of equation (6), we have calculated the relaxation time as a function of temperature for the semi-crystalline poly(ethylene terephthalate) (PET), and then compared with the experimental data reported in Ref. [50]. The obtained analytical results are shown in Figure (2). The volume fractions of mobile amorphous components in the PETs are 39.1%, 57.5% and 100%, respectively. The values of all the parameters of equation (6) are listed in Table 1. At 330 K, both the analytical and experimental results show that the relaxation time is increased from 141 s, 9710 s to 43744 s, with a decrease in the volume fraction of the mobile amorphous component from 100%, 57.5% to 39.1%. It is found that the relaxation motion is seriously restricted by decreasing the volume fraction of mobile amorphous component, whereas the volume fraction of crystalline component is therefore increased in the PET. As discussed above, there are cooperative relaxation motions between the mobile amorphous and crystalline components, resulted from their CRRs and cooperative phase transitions based on the Adam-Gibbs theory [30]. Therefore, the relaxation time of the semi-crystalline PET is then increased with an increase in the volume fraction of crystalline component.

[Table 1]

[Figure 2]

Based on the equation (8), we can investigate the effect of volume fraction of mobile amorphous component (W_m) on the phase evolution function (ϕ_m) as a function of temperature. As shown in Figure 3(a), the phase evolution function (ϕ_m) is

gradually decreased with an increase in temperature. Results show that the semi-crystalline SMPs can complete the phase transition (where ϕ_m=0) at 368 K, 372 K, 377 K, 382 K and 385 K, with a decrease in volume fraction from 95%, 90%, 85%, 80% to 75%. In these cases, the heating rate (q=2 K/min) and internal time (τ_0=2 min) are kept constants. These analytical results reveal that a higher temperature is needed to help the semi-crystalline SMP to complete the phase transition according to the equation (2), while simultaneously the volume fraction (W_m=1-λ) of mobile amorphous component is decreased and the volume fraction ($W_c = \lambda\varphi$) of crystalline component is increased.

On the other hand, the simulation results of temperature-dependent phase transition of the semi-crystalline SMPs are also plotted in Figure 3(b). It is found that the heating rate (q) plays a critical role to influence the phase transition, e.g., the phase evolution function is increased to a larger value at the same temperature when the heating rate is increased. The SMPs complete their phase transitions at 382 K, 395 K, 407 K, 410 K and 428 K, when the heating rates are set as 2 K/min, 5 K/min, 15 K/min and 20 K/min. The results reveal that the phase transition of semi-crystalline SMPs is prolonged with an increase in the heating rate, at the same volume fraction of mobile amorphous component of W_m=80%.

[Figure 3]

3.2 Experimental verification of epoxy/PCL triple-SMP

All the values of parameters used to predict the free recovery behavior are determined by the experimental data of the storage modulus of

epoxy/polycaprolactone SMP and semi-crystalline PLLA/PDLA/PU SMP (PU: polyurethane) [17,34], respectively. The universal global algorithm (UGO) method is adopted to determine the values of parameters used in the proposed models of equations (16) and (18). The convergence tolerance is set as 10^{-10}, and the maximum iteration is set as 2000.

All the values of parameters used to predict recovery behaviors of epoxy/PCL SMP are needed to determine by the dynamic thermomechanical analysis test. We have calculated the moduli results of the semi-crystalline epoxy/PCL and amorphous epoxy SMPs using equation (16), and the obtained results are compared with the experimental data reported in Ref. [34]. The values of parameters used in equation (16) are presented in Table 2.

[Table 2]

As shown in Figure 4, the storage modulus of the amorphous epoxy SMP is gradually decreased from 1345 MPa to 6.1 MPa with an increase in temperature from 295 K to 320 K, mainly due to the differences in the glass transitions. On the other hand, the storage modulus of semi-crystalline epoxy/PCL SMP is decreased from 1345 MPa to 19 MPa owing to the differences in the glass transitions of amorphous epoxy components. Results also present that the storage modulus is further decreased from 19 MPa to 4 MPa with the temperature increased from 335 K to 360 K, mainly due to the differences in the melting transitions of crystalline PCL components. The triple-SME and two-step recovery are both characterized and predicted using our newly proposed model, and the fitting curves are in good agreements with the

experimental data of semi-crystalline epoxy/PCL SMP [34], as shown in Figure 4.

[Figure 4]

3.3 Experimental verification of PLLA/PDLA/PU quadruple-SMP

Furthermore, the semi-crystalline PLLA/PDLA/PU SMP can reveal two glass transitions and two melting transitions, enabling a quadruple-SME. The Takayanagi principle [32] is employed to characterize the morphology feature of semi-crystalline PLLA/PDLA/PU SMP, and the obtained results are shown in Figure 5(a). The symbols of M1, R1 and C1 represent the mobile amorphous component, rigid amorphous component and crystalline component of PLLA segment, respectively. While symbols of M2, R2 and C2 represent the mobile amorphous component, rigid amorphous component and crystalline component of PDLA segment, respectively.

The analytical results of storage moduli obtained using the proposed model of equation (18) for the semi-crystalline PLLA/PDLA/PU SMP have been plotted in Figure 5(b), which has also included the experimental data obtained from the Ref. [17] for comparisons. Fitting values of parameters used in equation (18) are listed in Table 3. It is found that the analytical results are in good agreement with the experimental ones. The storage modulus is sequentially decreased from 2149 MPa to 78 MPa due to the glass transitions of PLLA segment; from 78 MPa to 20 MPa due to the glass transition of PDLA segment; from 20 MPa to 5.3 MPa due to the melting transition of PLLA segment; and from 5.3 MPa to 0.33 MPa due to the melting transition of PDLA segment. Clearly, the SMP presents a quadruple-SME and achieves a four-step recovery behavior with an increase in temperature.

[Table 3]

[Figure 5]

3.4 Dynamic mechanical behavior in triple-SMP

Using equation (12) and parameters listed in Table 2, we have calculated the stored strains ($\varepsilon_s(T,t)$) of semi-crystalline epoxy/PCL SMPs with triple-SME, and then compared with those experimental data reported in Ref. [34]. These results are plotted in Figure 6. The T_g of epoxy component is 303 K and the T_m of PCL crystalline component is 337 K. As shown in Figure 6(a), the epoxy part acts as the mobile amorphous and rigid amorphous components. While the PCL acts as the crystalline component. Since the T_g of epoxy component is lower than the T_m of PCL crystalline component, the glass transition is firstly achieved at 303 K during the heating process. Then the melting transition is achieved at 337 K. Therefore, there is a triple-SME (or a two-step recovery) generated in the epoxy/PCL SMPs [51].

Figure 6(b) plots the analytical results of the stored strains as a function of temperature for the semi-crystalline epoxy/PCL SMP using parameters in Table 2. The experimental data reported in Ref. [34] and the analytical results of previous model [26] were also collected and plotted for comparisons. It is found that the analytical results obtained from the proposed model are in well agreement with the experimental ones. The semi-crystalline epoxy/PCL SMP undergoes the glass transition and the first shape recovery of mobile amorphous epoxy component in the temperature range from 285 K to 318 K. Then the melting transition and the second shape recovery of crystalline PCL component are achieved in the temperature range from 329 K to 345

K. There is a plateau region located at the temperature range from 318 *K* to 329 *K* between the first and second shape recoveries.

It should be noted that the first glass transition of epoxy component is resulted from the cooperative relaxation motions of both mobile amorphous and crystalline components, according to the Adam-Gibbs theory [30]. Their CRRs are characterized by the rigid amorphous component in the proposed model, of which the analytical results are more suitable to predict the experimental data in comparison with those based on the previous model. Furthermore, the effect of volume fraction (W_m) of mobile amorphous epoxy component on the shape recovery behavior of semi-crystalline epoxy/PCL SMP has been investigated using equation (12), and the results are shown in Figure 6(c). Based on these analytical results, the SMPs complete their glass transitions at temperatures of 338.6 K, 329 K, 326 K, 322 K and 314 K, respectively, when the volume fractions of mobile amorphous epoxy components are increased from 0%, 10%, 15%, 20% to 25%. These analytical results reveal that the two-step shape recovery is also determined by the volume fractions of amorphous and crystalline components [34]. Furthermore, the triple-SME and shape recovery behavior can be designed and tailored by varying volume fractions of amorphous and crystalline components in the semi-crystalline epoxy/PCL SMP.

[Figure 6]

3.5 Dynamic mechanical behavior in quadruple-SMP

Equation (17) is employed to calculate the stored strains of the PLLA/PDLA/PU SMP with quadruple-SME using parameters in Table 3, and the obtained analytical

results are plotted and compared with the experimental data reported in Ref. [17]. Experimental results in Figure 7 revealed that the glass and melting transitions of PLLA and PDLA segments are able to store the temporary shapes in the semi-crystalline PLLA/PDLA/PU SMPs. As revealed in Figure 7, the first shape recovery of SMP is induced by the glass transition of PLLA component in the temperature range from 293 *K* to 333 *K*. The second shape recovery is triggered due to the melting transition of PLLA component in the temperature range from 333 *K* to 363 *K*. The third shape recovery is resulted from the melting transition of PDLA component in the temperature range from 363 *K* to 403 *K*. Therefore, a quadruple-SME has been achieved for the semi-crystalline PLLA/PDLA/PU SMP, whereas it takes 16 min, 32.5 min and 19.5 min to complete the three-step recovery processes.

[Figure 7]

3.6 Experimental verification of TME in semi-crystalline SMP

Effects of deformation temperature and mechanical loading stress on the TME have been investigated for the semi-crystalline PLLA/PDLA/PU SMPs, and the obtained results are shown in Figures 8(a), 8(b) and 8(c). The deformation temperatures are T_d =363 K, 373 K and 383 K, and the mechanical loading stresses are σ =1.15MPa, 1.3 MPa, and 1.4 MPa. Values of parameters used in equation 23(a) and 23(b) in the calculation are listed in Table 3. The experimental data reported in Ref. [17] for the semi-crystalline PLLA/PDLA/PU SMPs have been employed for comparison and verification. As shown in Figure 8(d), these analytical results predict well with the

experimental ones, and the degree of divergence between the analytical and experimental ones [17] are 9.92%, 8.3% and 5.2% at various deformation temperatures of T_d=363 K, 373 K and 383 K, respectively,. The analytical and experimental results reveal that the stored mechanical energy, which is influenced by both the deformation temperature and mechanical loading stress, plays an essential role to determine the TME in the semi-crystalline PLLA/PDLA/PU SMP. Therefore, both the deformation temperature and mechanical loading stress has a direct effect on the stored mechanical energy, of which the SME has the same working mechanism as that of the TME in the other types of SMPs [43,44].

[Figure 8]

4. Conclusions

In this study, a 1D multi-modal dynamic model based on three-phase model and Takayanagi principle was developed to describe the cooperative dynamics and thermomechanical behavior of the semi-crystalline SMPs with the multi-SME and TME. The cooperative dynamics and motions of amorphous and crystalline components have been formulated using the extended Adam-Gibbs theory and three-phase model. The phase transition theory and the modified Avrami theory have then been applied to characterize the glass and melting transitions, respectively. Furthermore, the commutative glass and melting transitions have been introduced into the SMPs, and the predictions of triple-SME, quadruple-SME and quintuple-SME have been achieved. The constitutive relationships of these multi-SME in the semi-crystalline SMPs have been modelled and verified by the experimental results.

Finally, the accuracy of analytical results is examined using experimentally obtained relaxation and thermomechanical behaviors reported in the literature, in order to verify the applicability and effectivity of the proposed model. This study is expected to provide a theoretical approach to explore the working principle and cooperative dynamics of multi-SME in semi-crystalline SMP, which provide guidelines for designing desirable relaxation and thermomechanical behaviors for the SMPs.

Acknowledgements

This work was financially supported by the National Natural Science Foundation of China (NSFC) under Grant No. 11725208 and UK Newton Mobility Grant (IE161019) through Royal Society and NFSC.

References

[1] Li J, Liu T, Xia S, Pan Y, Zheng Z, Ding X and Peng Y 2011 A versatile approach to achieve quintuple-shape memory effect by semi-interpenetrating polymer networks containing broadened glass transition and crystalline segments *J. Mater. Chem.* **21** 12213–7

[2] Lendlein A and Gould O E C 2019 Reprogrammable recovery and actuation behaviour of shape-memory polymers *Nat. Rev. Mater.* **4** 116–33

[3] Wang X, Liu Y, Lu H and Fu Y Q 2019 On the free-volume model of multi-shape memory effect in amorphous polymer *Smart Mater. Struct.* **28** 125012

[4] Charles A D M, Rider A N, Brown S A and Wang C H 2020 Improving the actuation performance of magneto-polymer composites by silane functionalisation of carbonyl-iron particles *Compos. Part B Eng.* **196** 108091

[5] Sabzi M, Babaahmadi M and Rahnama M 2017 Thermally and electrically

triggered triple-shape memory behavior of poly(vinyl acetate)/poly(lactic acid) due to graphene-induced phase separation *ACS Appl. Mater. Interfaces* **9** 24061–70

[6] Lu H, Gou J, Leng J and Du S 2011 Magnetically aligned carbon nanotube in nanopaper enabled shape-memory nanocomposite for high speed electrical actuation *Appl. Phys. Lett.* **98** 1–4

[7] Baniasadi M, Foyouzat A and Baghani M 2020 Multiple Shape memory effect for smart helical springs with variable stiffness over time and temperature *Int. J. Mech. Sci.* **182** 105742

[8] Zhang Y F, Zhang N, Hingorani H, Ding N, Wang D, Yuan C, Zhang B, Gu G and Ge Q 2019 Fast-response, stiffness-tunable soft actuator by hybrid multimaterial 3D printing *Adv. Funct. Mater.* **29** 1–9

[9] Baniasadi M, Yarali E, Foyouzat A and Baghani M 2021 Crack self-healing of thermo-responsive shape memory polymers with application to control valves, filtration, and drug delivery capsule *Eur. J. Mech. A/Solids* **85** 104093

[10] Peterson G I, Childers E P, Li H, Dobrynin A V. and Becker M L 2017 Tunable shape memory polymers from α-amino acid-Based poly(ester urea)s *Macromolecules* **50** 4300–8

[11] Xiao R, Guo J, Safranski D L and Nguyen T D 2015 Solvent-driven temperature memory and multiple shape memory effects *Soft Matter* **11** 3977–85

[12] Lu H, Wang X, Yu K, Fu Y Q and Leng J 2019 A thermodynamic model for tunable multi-shape memory effect and cooperative relaxation in amorphous polymers *Smart Mater. Struct.* **28** 025031

[13] Zhou J, Li Q, Turner S A, Ashby V S and Sheiko S S 2015 Isothermal programming of triple shape memory *Polymer* **72** 464–70

[14] Li J, Liu T, Xia S, Pan Y, Zheng Z, Ding X and Peng Y 2011 A versatile approach to achieve quintuple-shape memory effect by semi-interpenetrating polymer networks containing broadened glass transition and crystalline segments *J. Mater. Chem.* **21** 12213–7

[15] Nöchel U, Reddy C S, Uttamchand N K, Kratz K, Behl M and Lendlein A 2013

Shape-memory properties of hydrogels having a poly(ε-caprolactone) crosslinker and switching segment in an aqueous environment *Eur. Polym. J.* **49** 2457–66

[16] Bellin I, Kelch S, Langer R and Lendlein A 2006 Polymeric triple-shape materials *Proc. Natl. Acad. Sci. U. S. A.* **103** 18043–7

[17] Zhou J, Cao H, Chang R, Shan G, Bao Y and Pan P 2018 Stereocomplexed and homochiral polyurethane elastomers with tunable crystallizability and multishape memory effects *ACS Macro Lett.* **7** 233–8

[18] Li Y and Liu Z 2018 A novel constitutive model of shape memory polymers combining phase transition and viscoelasticity *Polymer* **143** 298–308

[19] Wang X, Lu H, Fu Y Q, Leng J and Du S 2020 Collective and cooperative dynamics in transition domains of amorphous polymers with multi-shape memory effect *J. Phys. D. Appl. Phys.* **53** 095301

[20] Diani J, Gilormini P, Frédy C and Rousseau I 2012 Predicting thermal shape memory of crosslinked polymer networks from linear viscoelasticity *Int. J. Solids Struct.* **49** 793–9

[21] Wang X, Lu H, Wu N, Hui D, Chen M and Fu Y Q 2019 Cooperative principle in multiple glass transitions and strain relaxations of thermochemically responsive shape memory polymer *Smart Mater. Struct.* **28** 085011

[22] Wunderlich B 2005 Effect of decoupling of molecular segments, microscopic stress-transfer and confinement of the nanophases in semicrystalline polymers *Macromol. Rapid Commun.* **26** 1521–31

[23] Hong P Da, Chuang W T, Yeh W J and Lin T L 2002 Effect of rigid amorphous phase on glass transition behavior of poly(trimethylene terephthalate) *Polymer* **43** 6879–86

[24] Jäckle J 1986 Models of the glass transition *Reports Prog. Phys.* **49** 171–231

[25] Hamonic F, Prevosto D, Dargent E and Saiter A 2014 Contribution of chain alignment and crystallization in the evolution of cooperativity in drawn polymers *Polymer* **55** 2882–9

[26] Ge Q, Luo X, Iversen C B, Mather P T, Dunn M L and Qi H J 2013 Mechanisms of triple-shape polymeric composites due to dual thermal transitions *Soft Matter* **9**

2212–23

[27] Ge Q, Luo X, Iversen C B, Nejad H B, Mather P T, Dunn M L and Jerry Qi H 2014 A finite deformation thermomechanical constitutive model for triple shape polymeric composites based on dual thermal transitions *Int. J. Solids Struct.* **51** 2777–90

[28] Moon S, Rao I J and Chester S A 2016 Triple shape memory polymers: constitutive modeling and numerical simulation *J. Appl. Mech. Trans. ASME* **83** 1–18

[29] Adam G and Gibbs J H 1965 On the temperature dependence of cooperative relaxation properties in glass-forming liquids *J. Chem. Phys.* **43** 139–46

[30] Matsuoka S 1997 Entropy, free volume, and cooperative relaxation *J. Res. Natl. Inst. Stand. Technol.* **102** 213-28

[31] Avrami M 1939 Kinetics of phase change. I: General theory *J. Chem. Phys.* **7** 1103–12

[32] Dickie R A 1973 Heterogeneous polymer–polymer composites. I. Theory of viscoelastic properties and equivalent mechanical models *J. Appl. Polym. Sci.* **17** 45–63

[33] Lu H, Wang X, Xing Z and Fu Y Q 2019 A cooperative domain model for multiple phase transitions and complex conformational relaxations in polymers with shape memory effect *J. Phys. D. Appl. Phys.* **52** 245301

[34] Luo X and Mather P T 2010 Triple-shape polymeric composites (TSPCs) *Adv. Funct. Mater.* **20** 2649–56

[35] Jonas A and Legras R 1993 Relation between PEEK semicrystalline morphology and its subglass relaxations and glass transition *Macromolecules* **26** 813–24

[36] Delpouve N, Saiter A, Mano J F and Dargent E 2008 Cooperative rearranging region size in semi-crystalline poly(l-lactic acid) *Polymer* **49** 3130–5

[37] Pak J, Pyda M and Wunderlich B 2003 Rigid amorphous fractions and glass transitions in poly(oxy-2,6-dimethyl-1,4-phenylene) *Macromolecules* **36** 495–9

[38] Liu Y, Gall K, Dunn M L, Greenberg A R and Diani J 2006 Thermomechanics of shape memory polymers: Uniaxial experiments and constitutive modeling *Int. J.*

Plast. **22** 279–313

[39] Curro J G, Lagasse R R and Simha R 1982 Diffusion model for volume recovery in glasses *Macromolecules* **15** 1621–6

[40] Jeziorny A 1978 Parameters characterizing kinetics of nonisothermal crystallization of poly(ethylene-terephthalate) determined by DSC *Polymer* **19** 1142–4

[41] Yang Q and Li G 2016 Temperature and rate dependent thermomechanical modeling of shape memory polymers with physics based phase evolution law *Int. J. Plast.* **80** 168–86

[42] Brinson H F 2007 Polymer Engineering Science and Viscoelasticity: An Introduction *Springer, New York.*

[43] Sun L and Huang W M 2010 Mechanisms of the multi-shape memory effect and temperature memory effect in shape memory polymers *Soft Matter* **6** 4403–6

[44] Xie T, Page K A and Eastman S A 2011 Strain-based temperature memory effect for Nafion and its molecular origins *Adv. Funct. Mater.* **21** 2057–66

[45] Westbrook K K, Kao P H, Castro F, Ding Y and Jerry Qi H 2011 A 3D finite deformation constitutive model for amorphous shape memory polymers: A multi-branch modeling approach for nonequilibrium relaxation processes *Mech. Mater.* **43** 853–69

[46] Laiarinandrasana L, Klinkova O, Nguyen F, Proudhon H, Morgeneyer T F and Ludwig W 2016 Three dimensional quantification of anisotropic void evolution in deformed semi-crystalline polyamide 6 *Int. J. Plast.* **83** 19–36

[47] Thévenon A and Fulchiron R 2014 A thermomechanical modeling approach of the structural changes in semi-crystalline polymers under elongational strain *J. Mater. Sci.* **49** 433–40

[48] Zeng F, Le Grognec P, Lacrampe M F and Krawczak P 2010 A constitutive model for semi-crystalline polymers at high temperature and finite plastic strain: Application to PA6 and PE biaxial stretching *Mech. Mater.* **42** 686–97

[49] Gueguen O, Richeton J, Ahzi S and Makradi A 2008 Micromechanically based formulation of the cooperative model for the yield behavior of semi-crystalline

polymers *Acta Mater.* **56** 1650–5

[50] Alves N M, Mano J F, Balaguer E, Meseguer Dueñas J M and Gómez Ribelles J L 2002 Glass transition and structural relaxation in semi-crystalline poly(ethylene terephthalate): A DSC study *Polymer* **43** 4111–22

[51] Yu K, Xie T, Leng J, Ding Y and Qi H J 2012 Mechanisms of multi-shape memory effects and associated energy release in shape memory polymers *Soft Matter* **8** 5687–95

Tables captions

Table 1. Values of parameters used in equation (6) for relaxation time of semi-crystalline PETs.

Table 2. Values of parameters for the semi-crystalline epoxy/PCL SMP.

Table 3. Values of parameters for the PLLA/PDLA/PU quadruple-SMP.

Table 1.

W_m (%)	T_g (K)	N	$\Delta C_{p0}(J/(g\cdot K))$	τ^* (min)	T^* (K)
39.1	365	7.2×10^{23}	0.33	1.0×10^{-5}	750
57.5	360	1.2×10^{24}			
100	338	9.3×10^{23}			

Table 2.

	Parameter	Value	Description
Mobile amorphous component (epoxy)	$E_{m,f}(MPa)$	1459.3	Modulus of frozen phase in the mobile amorphous component
	$E_{m,a}(MPa)$	6.1	Modulus of active phase in the mobile amorphous component
	$E_{r0}(MPa)$	1287.7	Modulus of rigid amorphous component
	$T_g(K)$	303.5	Glass transition temperature
	$T_0(K)$	288.3	Low-temperature limit
	$\tau_0(\min)$	0.6	Internal time
	$\Delta\mu N/\Delta C_{p0}$	2335.1	Fitting constant
Crystalline component (PCL)	$E_{c0}(MPa)$	1407.4	Modulus of the crystalline component
	$K_{\max}$	1.2	Maximum value of kinetic parameter
	$T_m(K)$	337.4	Melting transition temperature
	D	37.8	Fitting constant

Component composition	α	0.47	Fitting constant
	λ	0.68	The dimensionless width of crystalline component along the loading direction
	φ	0.36	The dimensionless length of crystalline component along the loading direction

Table 3.

Parameter	λ	α	$E_{m,f}$ (MPa)	$E_{m,a}$ (MPa)	T_0 (K)	τ_0 (min)	$T_g(K)$	$N\Delta\mu/W_m\Delta C_{p0}$
Glass transition of PLLA	0.1	0.99	3158.6	7.1	218	5.75	223	598.07
Glass transition of PDLA	0.4	1.01	2557.6	5.6	255.8	4.58	253	153.62

Parameter	λ	φ	E_{c0} (MPa)	E_{r0} (MPa)	T_m (K)	D	K_{max}	$\sigma_i(0)$ (MPa)	T^* (K)	μ_c (MPa)
Melting transition of PLLA	0.2	0.58	3002.3	2425.7	360	798	0.03	1.6	620	2.1
Melting transition of PDLA	0.3	0.73	3233.4	2677.8	400	382	0.05	3.2	710	2.4

Figures captions

Figure 1. Illustration of three-phase feature in a semi-crystalline SMP composed of mobile amorphous, rigid amorphous and crystalline components, based on the three-phase model [22].

Figure 2. Comparisons between analytical results using the equation (6) and experimental data of relaxation time as a function of temperature for semi-crystalline PETs, as reported in Ref. [50].

Figure 3. Phase evolution function (ϕ_m) as a function of temperature. (a) At various volume fraction of mobile amorphous component of W_m=75%, 80%, 85%, 90% and 95%. (b) At various heating rates of q=2 K/min, 5 K/min, 10 K/min, 15 K/min and 20 K/min.

Figure 4. Comparisons between analytical results of equation (16) and the experimental data reported in Ref. [34] of amorphous epoxy and semi-crystalline epoxy/PCL SMPs.

Figure 5. (a) Illustration of the morphology feature of semi-crystalline PLLA/PDLA/PU SMP undergoing two glass and two melting transitions, based on the Takayanagi principle [32]. (b) Comparison between calculation results of equation (18) and experimental data [17] of the storage modulus as a function of temperature in semi-crystalline PLLA/PDLA/PU SMP.

Figure 6. (a) Illustrations of triple-SME in the semi-crystalline epoxy/PCL SMP, which is incorporated from mobile amorphous, rigid amorphous and crystalline components. (b) Comparisons among analytical results using equation (12), using the previous model [27], and experimental data [34] of the stored strain as a function of temperature for semi-crystalline epoxy/PCL SMP. (c) Analytical results of the stored strain as a function of temperature at various volume fraction of mobile amorphous component of W_m=0%, 10%, 15%, 20%, 25% to 100%.

Figure 7. Comparisons of stored strains with respect to recovery time between analytical results and experimental data [17] of semi-crystalline PLLA/PDLA/PU SMP with quadruple-SME.

Figure 8. Comparisons between analytical results obtained using the equation (23) and the experimental data [17] for the strain as a function of relaxation time. (a) At T_d =363 K and σ =1.4 MPa. (b) At T_d =373 K and σ =1.3 MPa. (c) At T_d =383 K and σ =1.15MPa. (d) the divergences between the analytical and experimental results at the temperatures of T_d =363K, 373K and 383K.

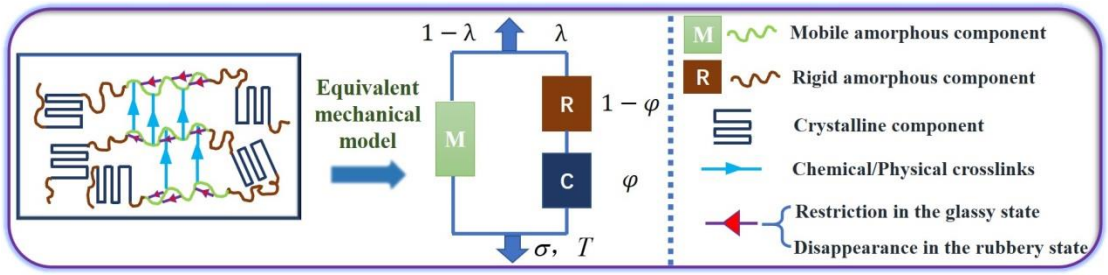

Figure 1.

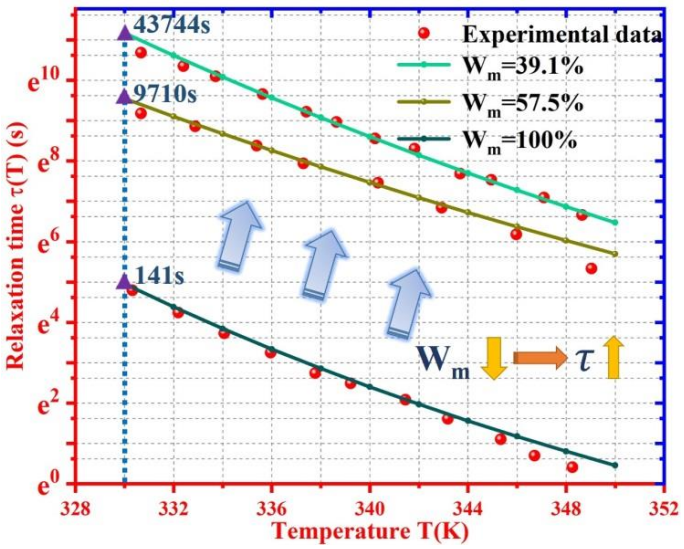

Figure 2.

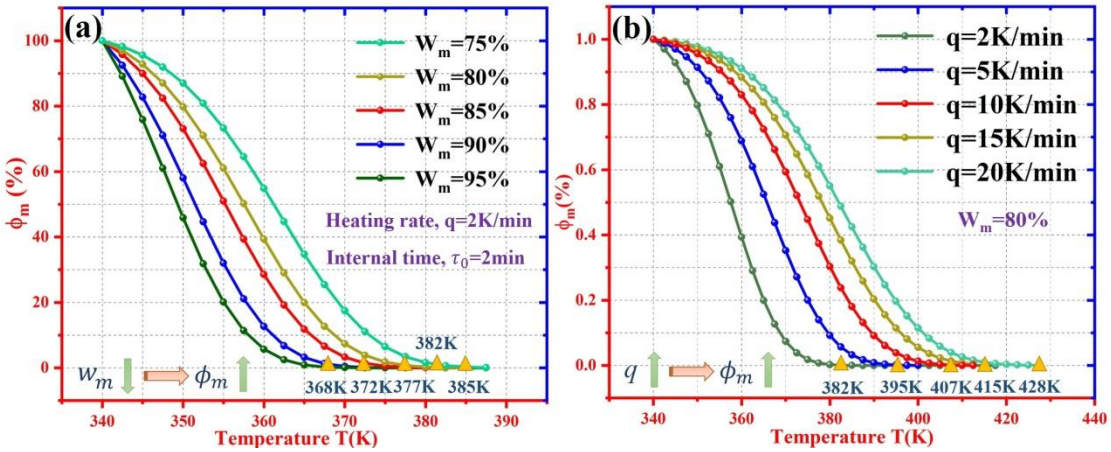

Figure 3.

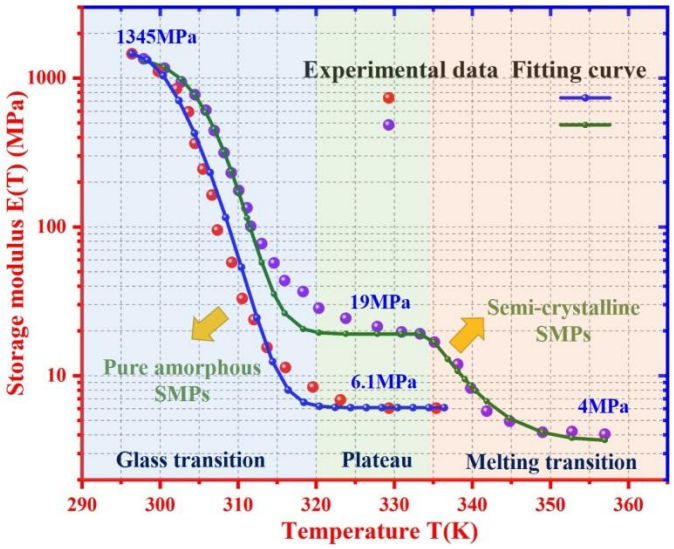

Figure 4.

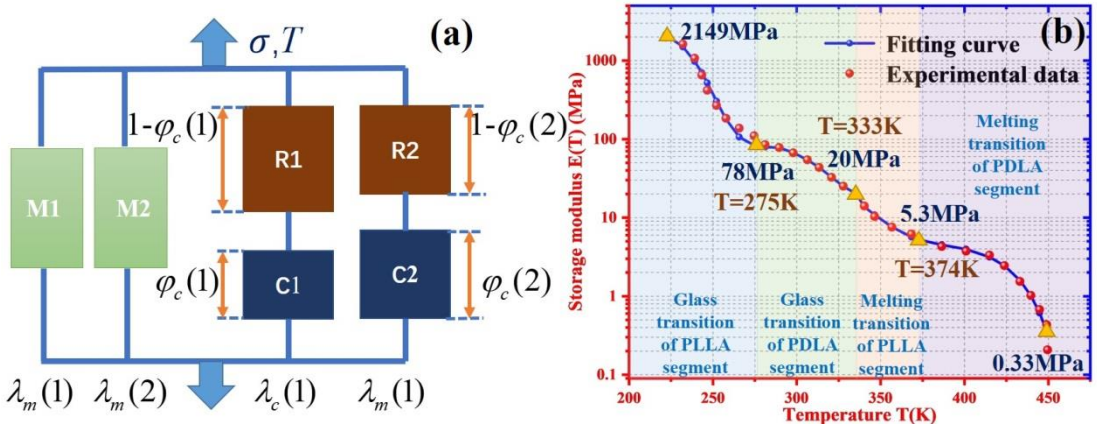

Figure 5.

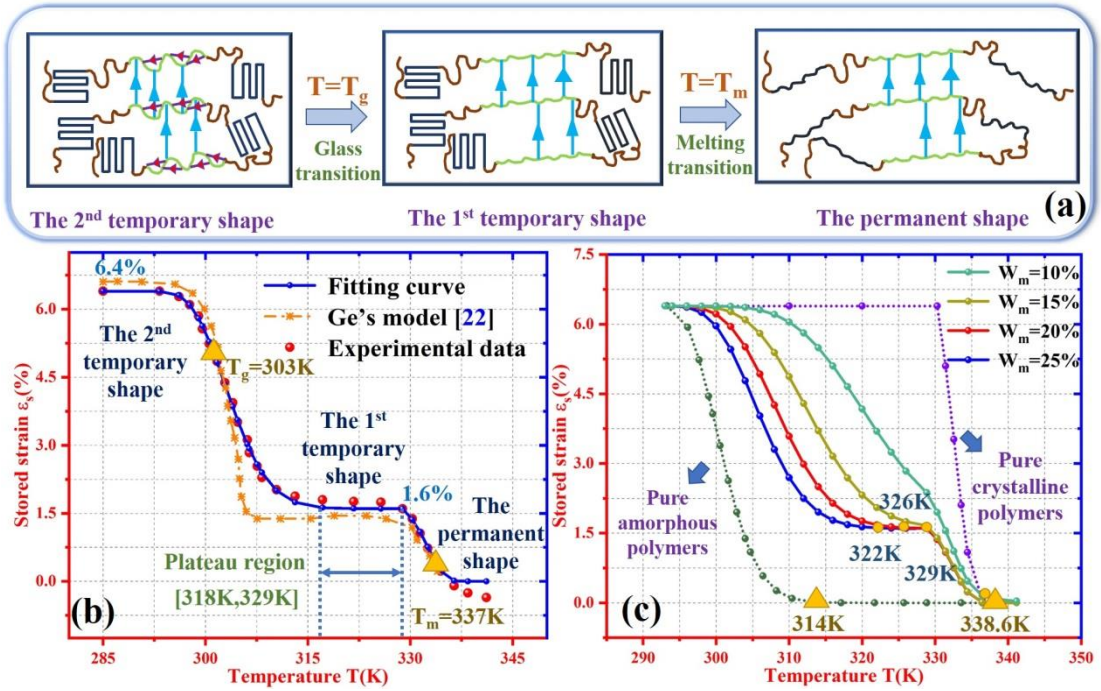

Figure 6.

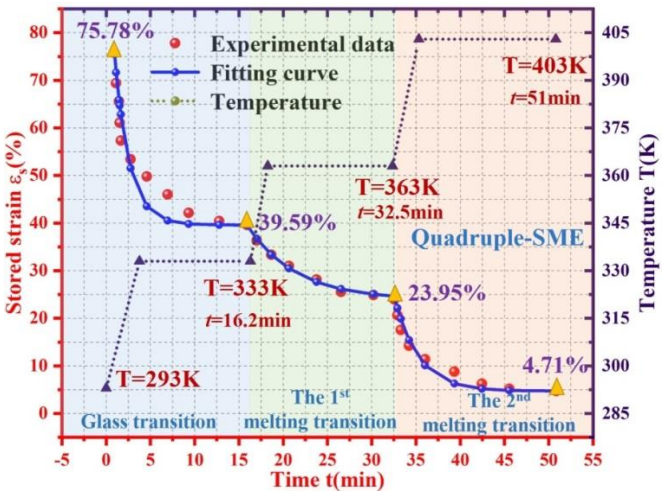

Figure 7.

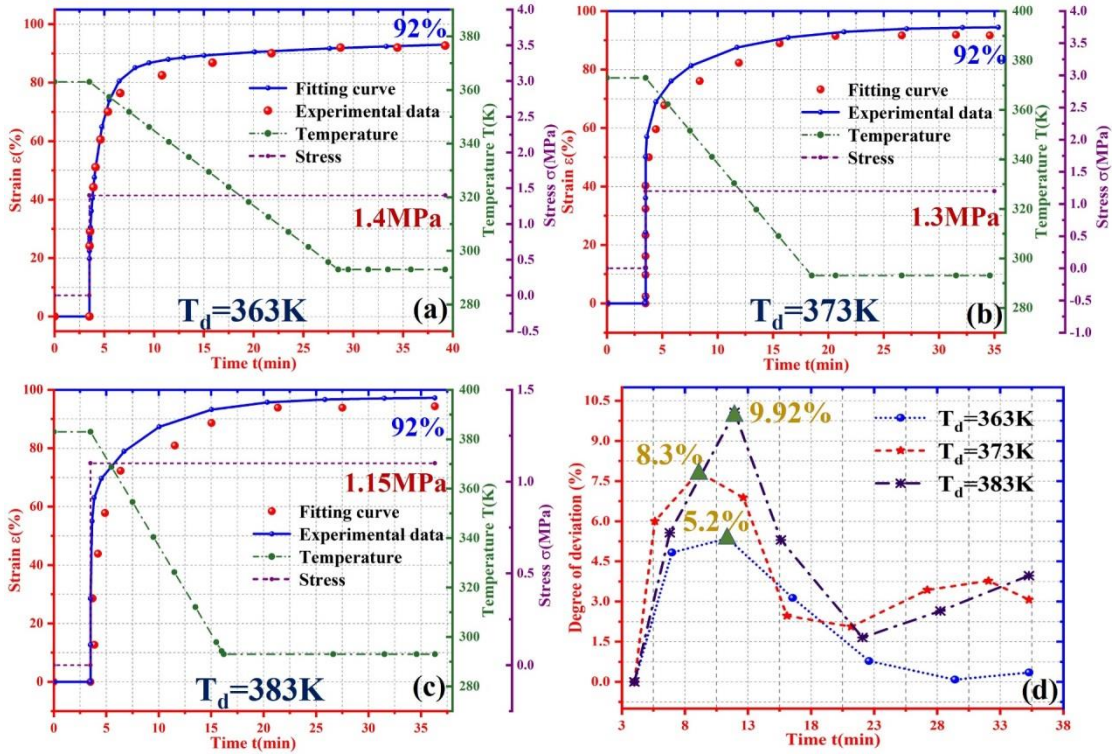

Figure 8.